PHYSICAL REVIEW D VOLUME 7, NUMBER 4 15 FEBRUARY 1973

# Analyiticity and Unitarity of Relativistic Off-Shell Models

J. V. Greenman
*Department of Mathematics, University of Essex, Colchester, Essex, England*
(Received 13 March 1972)

In this paper we discuss two questions concerning off-shell relativistic models not involving integration over relative energy: (i) Is it possible to obtain a unitary off-shell model with simple potential whose singularity structure is a reasonable approximation to that of Mandelstam? (ii) Is it possible to derive an off-shell model satisfying two- and three-body unitarity by a consistent procedure from a basic field-theory model? On the first point we analyze the singularity structure of three proposed models satisfying two-particle unitarity and show that their singularity structures deviate as much from the Mandelstam form as that of the Blankenbecler-Sugar equation. On the second point we generalize one of these two-particle models to incorporate three-particle unitarity, deriving the generalization from an analysis of the ladder-approximated dressed-rung Bethe-Salpeter equation.

## I. INTRODUCTION

The calculations of Aaron *et al.*[1] have shown that off-shell models can be a useful alternative to the $N/D$ approach. The major advantage of the off-shell models is that one can conveniently incorporate multiparticle unitarity. Most relativistic off-shell calculations involving two- and three-particle unitarity have been performed on models where the relative-energy integration has been removed.[1,2] Such models are in an essential way *ad hoc* in that to remove relative energy the Feynman three-particle Green's function is replaced by a generalized Blankenbecler-Sugar dispersive approximation,[3] whose justification in the first instance is convenience. The original Blankenbecler-Sugar equation[3] is just one of several proposed two-particle unitary off-shell models in which the relative energy has been removed. On one criterion at least, that of comparison with the ladder-approximated Bethe-Selpeter equation,[4] the Blankenbecler-Sugar equation is not the best model to use.[5] It seems worthwhile therefore to look at alternative prescriptions for removing relative energies in off-shell models satisfying both two- and three-particle unitarity. In Sec. IV we present one such alternative and show how it may be obtained by a consistent approximative procedure from a basic field-theoretic model, the ladder-approximated dressed-rung Bethe-Salpeter model.[6]

To the extent that one's confidence in a model relies on the successful building into the model of the correct analyticity properties, the off-shell models are to be found wanting. There is in fact a fundamental question of consistency since the inhomogeneous term of the off-shell model is normally chosen to correspond to the presumed closest crossed-channel singularity of the solution of the model. There is consistency in the original two-particle Blankenbecler-Sugar equation even though the singularity structure departs radically from that predicated by the Mandelstam representation. In fact complex singularities[7] are found to have moved onto the physical sheet. In partial-wave projection the distorted singularity structure shows up as an extra branch point on the left-hand branch cut.[3,7] Consistency does not, however, exist for other proposed models satisfying two-particle unitarity that we review in Sec. II and analyze in Sec. III. The variety of spurious singularities is much richer. Those close to the physical region happen to be quite weak compared to the $t$-channel particle pole a comparable distance away. Thus the distorted singularity structure does not significantly manifest itself in numerical calculation.[5] However, in certain calculations with two- and three-particle unitarity the spurious singularities have been found to give significant contributions.[8]

The analysis in Sec. III suggests that it is inevitable that spurious singularities will move onto the physical sheet whenever we insist on a Yukawa-type potential and no integration over relative energy, since removal of relative energy entails partially fractioning Feynman propagators and throwing away those terms that would cancel the spurious singularities generated in the fractioning process. By suitable choice of an energy-dependent potential one can remove the spurious singularities. This is clear in the case of the quasi-potential equation[9] since this equation can be derived from general field-theoretic considerations. Also, if for the energy-analytic model[10] discussed in Sec. II we take the potential to be a dispersed form of the solution of the ABFST (Amati, Bertocchi, Fubini, Stanghellini, and Tonin) equation[11] then we rederive the ladder-approximated Bethe-

Salpeter equation whose only analytic peculiarity is its bound-state spectrum.[12]

In summary, in Sec. II we review four off-shell models incorporating two-particle unitarity: (i) the Blackenbecler-Sugar quasipotential model,[3,9] (ii) the Gross model,[13] (iii) the energy-analytic model,[10] and (iv) the Cohen model.[5,14] In Sec. III we analyze the analyticity properties of the on-mass-shell second Born term of each of the four models. We restrict attention to these terms since the set of singularities of a second Born term is expected to appear in the full amplitude as the first set of a hierarchy of singularities. The other singularities, further from the physical region, can be obtained by iterating the equation. In Sec. IV we generalize the Gross model to incorporate both two- and three-particle unitarity.

Throughout the analysis we denote four-vectors by $p=(p_0, \vec{p})$ with metric $p^2=p_0{}^2-\vec{p}^2$. For simplicity in Secs. II and III we take the masses of all exchanged particles to be equal to $\mu$, and of all transmitted particles $m$. The particles will always be spinless.

## II. TWO-BODY OFF-SHELL MODELS

In this and the following section we discuss four models satisfying two-particle unitarity and defined by the following equations:

$$T(\hat{p}, \hat{q}_m)=T_0(\hat{p}, \hat{q}_m)+\lambda\int d^3k\{4(\vec{k}^2+m^2)^{1/2}D_0(\hat{p}, \hat{k})(\vec{q}_m{}^2-\vec{k}^2+i\epsilon)\}^{-1}T(\hat{k}, \hat{q}_m), \tag{1}$$

$$T(p_+, \hat{q}_m)=T_0(p_+, \hat{q}_m)+\lambda\int d^4k[D_0(p_+, k)D_-]^{-1}\delta^+(D_+)T(k_+, \hat{q}_m), \tag{2}$$

$$T(\hat{p}, \hat{q}_m)=T_0(\hat{p}, \hat{q}_m)+\frac{i\lambda}{2\pi}\int d^4k[D_0(\hat{p}, k)D_+D_-]^{-1}T(\hat{k}, \hat{q}_m), \tag{3}$$

$$\begin{aligned} T_\theta(p_\theta, \hat{q}_m)=T_0(p_\theta, \hat{q}_m)&+\lambda\int d^4k[(D^\theta_{0+}D_-)^{-1}\delta^+(D_+)-(D^\theta_{0-}D_+)^{-1}\delta^-(D_-)]T_+(k_+, \hat{q}_m)\\ &+\lambda\int d^4k[(D^\theta_{0+}D_+)^{-1}\delta^+(D_-)-(D^\theta_{0-}D_-)^{-1}\delta^-(D_+)]T_-(k_-, \hat{q}_m).\end{aligned} \tag{4}$$

The equations are written in the center-of-mass frame where the total incoming momentum has vector $E=(E, \vec{0})$. The momentum labeling in the equations is as follows:

$\hat{p}=(0, \vec{p})$,

$\phi^2=\frac{1}{4}E^2-m^2$,

$|\vec{p}_m|=\phi$,

$\hat{p}_m=(0, \vec{p}_m)$,

$P_{0\theta}=-\frac{1}{2}\theta E+(\vec{p}^2+m^2)^{1/2}$ ($\theta$ taking values $\pm1$),

$P_\theta=(P_{0\theta}, \vec{p})$,

$D_0(p, k)=(p-k)^2-\mu^2+i\epsilon$,

$D_\pm=(k_0\pm\frac{1}{2}E)^2-(\vec{k}^2+m^2)+i\epsilon$,

$\delta^\phi(D_\psi)=\theta(\phi(k_0+\frac{1}{2}\psi E))\,\delta(D_\psi)$ ($\phi, \psi$ taking values $\pm1$),

$D^\theta_{0\phi}(p_\theta, k)=2[(\vec{p}-\vec{k})^2+\mu^2]^{1/2}\{(p_{0\theta}-k_0)-\phi[(\vec{p}-\vec{k})^2+\mu^2]^{1/2}+\theta\phi i\epsilon\}$.

$T_0(p, \hat{q}_m)$ is the Born term $(2\pi)^3\lambda D_0{}^{-1}(p, \hat{q}_m)$. The on-mass-shell amplitude of Eqs. (1), (2), and (3) is $T(\hat{p}_m, \hat{q}_m)$, and that of Eq. (4) is $T_+(\hat{p}_m, \hat{q}_m)$. All these equations were derived as approximations to the ladder Bethe-Salpeter model defined by the equation

$$T(p, q)=T_0(p, q)+\frac{i\lambda}{2\pi}\int d^4k[D_0(p, k)D_+D_-]^{-1}T(k, q). \tag{5}$$

In fact if one uses an energy-analytic (EA) representation[15] in the relative and total incoming energy for the solution of Eq. (5) and retains contributions only from singularities closest to the physical region, one can obtain the quasipotential model [Eq. (1)]. If one uses an EA representation in just the relative incoming energy[10] and retains contributions from only the closest singularities in that variable then one obtains the EA model [Eq. (4)]. This latter model is likely to be a good approximation to Eq. (5) if $\mu/m \to \infty$. Gross[13] has considered the limit $\mu/m \to 0$ and obtained a model similar to that of Eq. (2). We have, for simplicity, dropped a crossed-box-graph contribution to the kernel of the integral equation, and to that extent the model of Eq. (2) is not consistent with the principle of retaining all terms of the first order in $\mu/m$. Nevertheless we call this the Gross model. The model of Eq. (3) is an *ad hoc* model proposed by Cohen[5] as an improvement on a previous idea of Cohen *et al.*[14]

The on-mass-shell second Born terms for the quasipotential (QP) and Cohen (CH) models are, respectively,

$$B_2^{QP} = (2\pi)^3\lambda^2\int d^3k\{4(\vec{k}^2+m^2)^{1/2}[(\vec{p}_m-\vec{k})^2+\mu^2](\vec{q}_m^{\,2}-\vec{k}^2+i\epsilon)[(\vec{k}-\vec{q}_m)^2+\mu^2]\}^{-1}, \tag{6}$$

$$B_2^{CH} = i(2\pi\lambda)^2\int d^4k\{[(\hat{p}_m-k)^2-\mu^2+i\epsilon][(k+\tfrac{1}{2}E)^2-m^2+i\epsilon][(k-\tfrac{1}{2}E)^2-m^2+i\epsilon][(\hat{k}-\hat{q}_m)^2-\mu^2+i\epsilon]\}^{-1}. \tag{7}$$

The Gross model is not time-reversal invariant. To make it so would require two coupled equations as in the EA model. The on-mass-shell Born term of this time-reversal invariant Gross model (GR) is given by

$$B_2^{GR} = B_2(E)+B_2(-E), \tag{8}$$

where

$$B_2(E) = (2\pi)^3\lambda^2\int d^3k\{4E\Omega_1[(\hat{p}_m-k_+)^2-\mu^2+i\epsilon][\tfrac{1}{2}E-\Omega_1][(k_+-\hat{q}_m)^2-\mu^2+i\epsilon]\}^{-1} \tag{9}$$

and $\Omega_1=(\vec{k}^2+m^2)^{1/2}$. The on-mass-shell second Born term of the EA model is

$$B_2^{EA} = \tilde{B}_2(E)+\tilde{B}_2(-E), \tag{10}$$

where $\Omega_0=[(\vec{p}_m-\vec{k})^2+\mu^2]^{1/2}$, $\Omega_2=[(\vec{q}_m-\vec{k})^2+\mu^2]^{1/2}$, and

$$\tilde{B}_2(E) = (2\pi)^3\lambda^2\int d^3k\{4E\Omega_1\Omega_0(\tfrac{1}{2}E-\Omega_1-\Omega_0)(\tfrac{1}{2}E-\Omega_1+i\epsilon)[(-\tfrac{1}{2}E+\Omega_1)^2-\Omega_2^{\,2}+i\epsilon]\}^{-1}. \tag{11}$$

The strategy we use to find the analyticity properties in $s$ and $t$ of these terms is to perform explicitly the angle integrations and then to look for pinching and end-point singularities in the $|\vec{k}|$ integration. This procedure is straightforward for the terms (6) and (9). For term (7) we have to perform a preparatory integration in $k_0$. We choose to do this in the following fashion: Writing $D_0(\hat{p}_m,k)$ as a sum of its positive- and negative-frequency parts the $k_0$ integral consists of two terms

$$\begin{aligned}&\int dk_0\{2\Omega_0(-k_0-\Omega_0+i\epsilon)[(k_0+\tfrac{1}{2}E)^2-\Omega_1^{\,2}+i\epsilon][(k_0-\tfrac{1}{2}E)^2-\Omega_1^{\,2}+i\epsilon]\}^{-1},\\ &-\int dk_0\{2\Omega_0(-k_0+\Omega_0-i\epsilon)[(k_0+\tfrac{1}{2}E)^2-\Omega_1^{\,2}+i\epsilon][(k_0-\tfrac{1}{2}E)^2-\Omega_1^{\,2}+i\epsilon]\}^{-1}.\end{aligned} \tag{12}$$

We evaluate the first (second) term in (12) by completing the contour in the lower (upper) half-plane. This yields the following expression for $B_2^{CH}$:

$$B_2^{CH} = B_2'(E)+B_2'(-E), \tag{13}$$

where

$$B_2'(E) = (-1)(2\pi)^3\lambda^2\int d^3k[4E\Omega_1\Omega_0(-\tfrac{1}{2}E+\Omega_1+\Omega_0)(\tfrac{1}{2}E-\Omega_1+i\epsilon)\Omega_2^{\,2}]^{-1}. \tag{14}$$

The structure of $B_2^{CH}$ is therefore similar to that of $B_2^{EA}$. The form of the integrand of (11) and (14) does not lead to a simple integration over the angle variables. To obviate this problem we use the following identity:

$$\frac{1}{y(x-y)} = \frac{2}{x^2-y^2}+\frac{x}{\pi}\int\frac{d\xi}{\sqrt{\xi}}\frac{1}{y^2+\xi}\frac{1}{x^2+\xi}, \tag{15}$$

with the identification $x=-k_0$, $y=\Omega_0-i\epsilon$. Substitution of this identity in (11) and (14) yields terms that are tractable.

The singularities of these four second Born terms are given in the next section.

## III. SECOND-BORN-TERM ANALYSIS

Analysis of the four integrals $B_2^{\rm QP}$, $B_2^{\rm GR}$, $B_2^{\rm CH}$, and $B_2^{\rm EA}$ is equivalent to the analysis of the following three integrals:

$$I_i(E)=\int d^3k(A_iB_iC_iD_i)^{-1}, \quad i=1,2,3 \qquad (16)$$

where $A_i$ is a kinematic factor, $B_i, D_i$ arise from the two Feynman exchange propagators, and $C_i^{-1}$ is a Green's function. These functions are specified in Table I.

For each of the integrals $I_i$ we perform[16] the angle integrations after introducing the Feynman parameter $\alpha$ such that

$$(B_iD_i)^{-1}=\tfrac{1}{2}\int_{-1}^{1}d\alpha[\tfrac{1}{2}(1+\alpha)B_i+\tfrac{1}{2}(1-\alpha)D_i]^{-2} \ . \qquad (17)$$

We are then left with two integrations, one over $\alpha$ and the other over, conveniently, $x\equiv 4(\vec{k}^2+m^2)$. The singularities of the $\alpha$ integral are determined by pinch analysis.[17]

For $i=1$ the positions of the $\alpha$ end-point singularities are given by

$$x=(s-4\mu^2)\pm 4i\mu(s-4m^2)^{1/2} \equiv x_\pm(s,0) \ , \qquad (18)$$

and of the $\alpha$ pinch singularity by

$$x=2t+s-4\mu^2\pm 2i[(4\mu^2-t)(t+s-4m^2)]^{1/2} \equiv x_\pm(s,t) \ . \qquad (19)$$

For fixed $t$, $x=x_\pm(s,t)$ provides us with two conformal mappings $s\to x$. In Fig. 1 we plot the image curves of the real axis of $s$ under these mappings for $t<4\mu^2$. It is clear from Fig. 1 that movement along the real $s$ axis does not lead to engagement of the singularity $x_+(s,t)$ with the $x$ contour of integration ($4m^2\leq {\rm Re}x<\infty$). This is in fact true; however, we move in the cut $s$ plane. However, for the singularity $x_-(s,t)$ there is always engagement with the $x$ contour provided we are sufficiently far to the left in the $s$ plane. The only pinch singularity of the $x$ integral that subsequently develops is with the kinematic singularity of $A_1$, at $x=0$. This singularity is located at

$$s=-4[\mu^2+m(4\mu^2-t)^{1/2}] \ . \qquad (20)$$

This is a singularity of $I_i$ generated from the $\alpha$ pinch singularity (19). The singularity of $I_1$ generated from the $\alpha$ end-point singularities (18) is located at

$$s=-4(\mu+2m)\mu \ . \qquad (21)$$

For $t>4\mu^2$ the singularity (20) moves into the complex plane and there is a further $x$ pinch singularity, namely with the Green's function pole $C_1^{-1}$ generating the normal Mandelstam singularity on the upper branch of the hyperbola

$$(s-4m^2)(t-4\mu^2)=4\mu^4 \ . \qquad (22)$$

$B_2^{\rm QP}$ is in fact proportional to $I_1$, and hence the singularities (20), (21), and (22) are possessed by $B_2^{\rm QP}$ in agreement with the analysis of Ref. 7. The singularities are plotted in Fig. 2(a), with the convention that complex singularities are represented by their projection in the Res-Ret plane.

TABLE I. Three sets of functions employed in the analysis of Eq. (16).

| $i$ | $A_i$ | $B_i$ | $C_i$ | $D_i$ |
|---|---|---|---|---|
| 1 | $(\vec{k}^2+m^2)^{1/2}$ | $(\vec{p}_m-\vec{k})^2+\mu^2$ | $\phi^2-\vec{k}^2+i\epsilon$ | $(\vec{q}_m-\vec{k})^2+\mu^2$ |
| 2 | $(\vec{k}^2+m^2)^{1/2}$ | $(\hat{p}_m-k_+)^2-\mu^2$ | $E[\frac{1}{2}E-\Omega_1+i\epsilon]$ | $(k_+-\hat{q}_m)^2-\mu^2$ |
| 3 | $(\vec{k}^2+m^2)^{1/2}$ | $(\vec{p}_m-\vec{k})^2+\mu^2$ | $E[\frac{1}{2}E-\Omega_1+i\epsilon]$ | $(k_+-\hat{q}_m)^2-\mu^2$ |

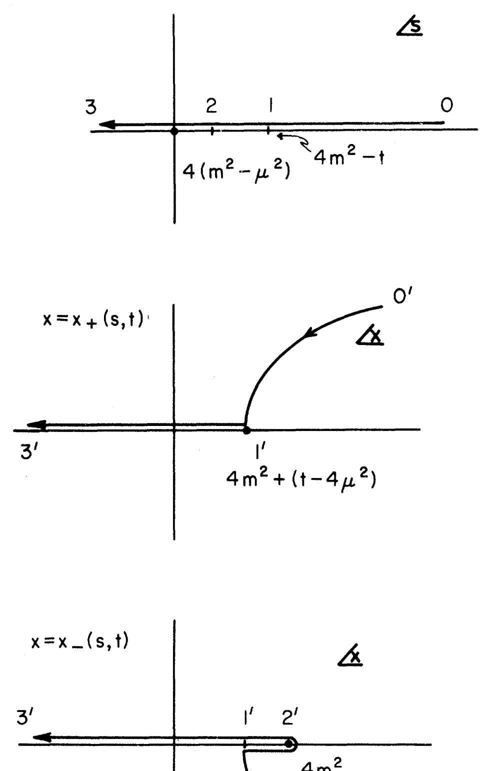


FIG. 1. Image of Res axis under conformal mappings $x=x_\pm(s,t)$ generated by the $\alpha$-pinch singularity of $I_1$.

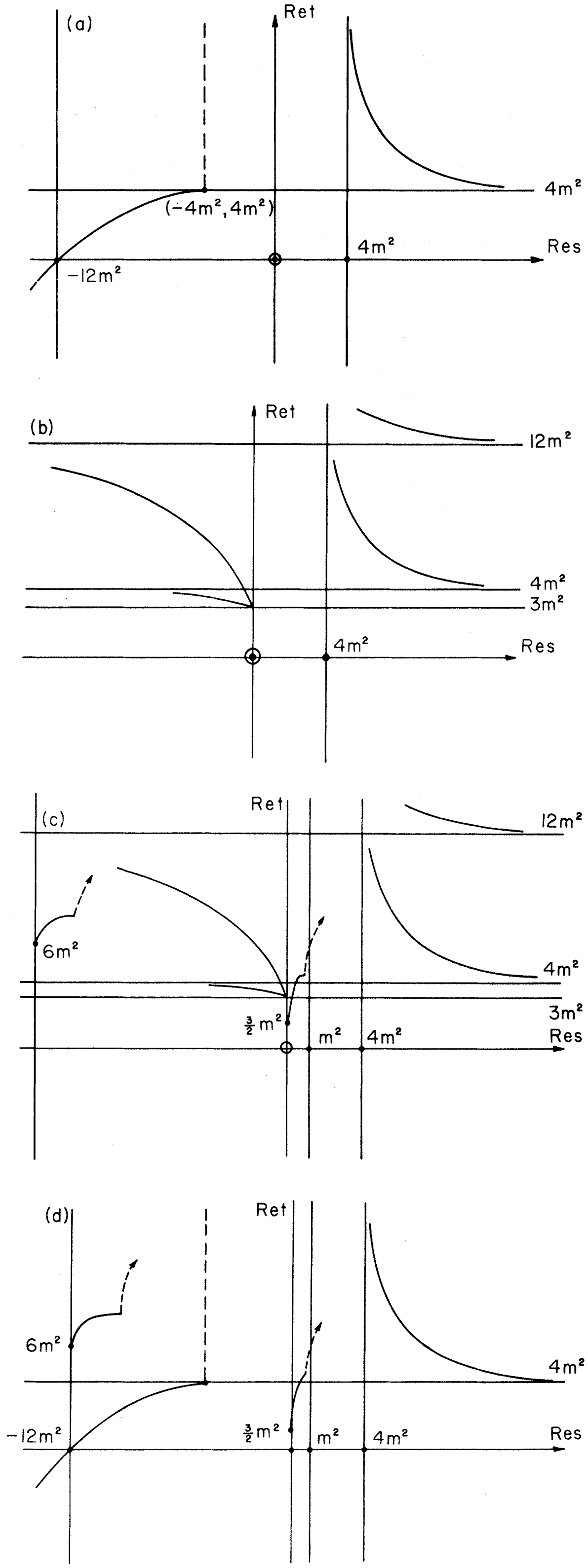


FIG. 2. The singularity structure, for $m=\mu$, of (a) $B_2^{\rm QP}$, (b) $B_2^{\rm GR}$, (c) $B_2^{\rm EA}$, and (d) $B_2^{\rm CH}$

Similarly one can show by standard methods[17] that the $\alpha$ end-point singularities of $I_2^+=I_2(E)+I_2(-E)$ are located at

$$2m^4x=\{[\mu^2(\mu^2-4m^2)(s-4m^2)]^{1/2}\pm(2m^2-\mu^2)s^{1/2}\}^2 \equiv 2m^4\tilde{x}_\pm(s,0)\ , \qquad (23)$$

and the $\alpha$ pinch singularity at

$$\tfrac{1}{4}(4m^2-t)^2x =\{[(\mu^2(\mu^2-4m^2)+m^2t)(s+t-4m^2)]^{1/2} \pm(2m^2-\mu^2)s^{1/2}\}^2 \equiv \tfrac{1}{4}(4m^2-t)^2\tilde{x}_\pm(s,t)\ . \qquad (24)$$

The images of the real $s$ axis under the conformal mappings $x=\tilde{x}_\pm(s,t)$ are plotted in Fig. 3 for $t<(4m^2-\mu^2)\mu^2/m^2$. It is the $\tilde{x}_-$ singularity that engages the integration contour and distorts it for $s$ past $m^2$. This distortion results in an inverse-square-root second-type singularity occurring on the physical sheet at $s=0$ due to confluence with

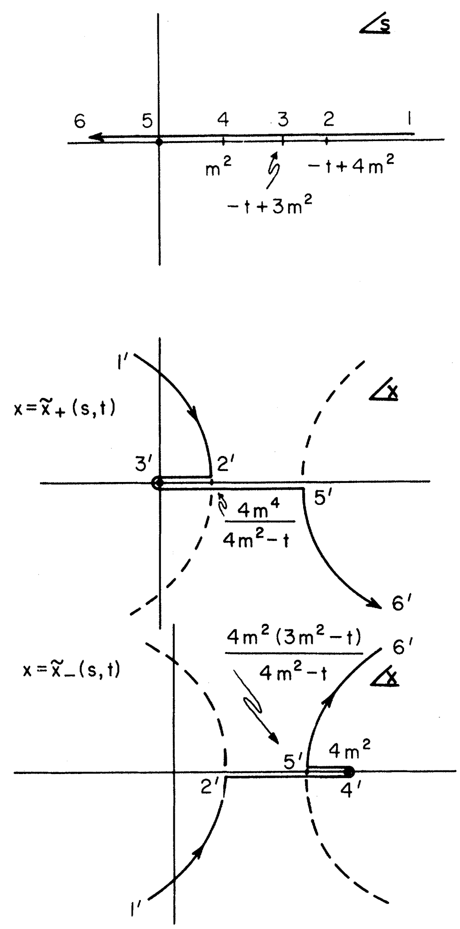


FIG. 3. Image of Res axis under conformal mappings $x=\tilde{x}_\pm(s,t)$ generated by the $\alpha$-pinch singularity of $I_2^+$.

$\bar{x}_+$. This and the $s$-channel elastic threshold branch branch point at $s=4m^2$ are the only singularities of the amplitude for $t<(4m^2-\mu^2)(\mu/m)^2 \equiv t_1$. When $t=t_1$ the singularities $\bar{x}_\pm$ coincide with the kinematic singularity at $x=0$ simultaneously with the Green's function pole at $s=x$. This confluence implies a branch point at $t=t_1$ through which emerge inverse-square-root singularities on the lower branches of the hyperbolas

$$(s-4m^2)[t-4(4m^2-\mu^2)]=4(4m^2-\mu^2)^2 , \quad (25a)$$

$$(s-4m^2)(t-4\mu^2)=4\mu^4 . \quad (25b)$$

There are also pinches between $\bar{x}_\pm$ and the Green's function pole on the undistorted contour of integration. These singularities are plotted in Fig. 2(b). Since $I_2^+$ is proportional to $B_2^{\mathrm{GR}}$ these are the singularities of $B_2^{\mathrm{GR}}$.

The integral $I_3^+ \equiv I_3(E)+I_3(-E)$ is a hybrid of the first two integrals $I_1^+, I_2^+$. The $\alpha$ end-point singularities are (18) and (23). The $\alpha$-pinch singularities are nontrivial to locate since there is no longer symmetry in $\alpha$. There is coincidence of poles in $\alpha$ when

$$\phi^2u^2+tu(v+\tfrac{1}{4}s)-t(v+\tfrac{1}{4}s)^2+vt(t+s-4m^2)=0, \quad (26)$$

where $u=k_0^{\,2}$, $v=k^2$. The constraint $k_0=\pm\frac{1}{2}s^{1/2}+(v+m^2)^{1/2}$ is equivalent to the relation

$$(u-v+\phi^2)^2-su=0 . \quad (27)$$

A solution of Eqs. (26) and (27) does not necessarily imply a pinch of the $\alpha$ contour. For fixed negative $t$ if we follow $s$, for example, through the physical $s$-channel region from large positive $s$ to the boundary at $s=4m^2-t$, a path is traced out in the $x=4(v+m^2)$ Argand plane derived from the condition of confluence of the two poles in the $\alpha$ plane. The confluence occurs at complex values of $\alpha$, moving in the limit at $s=4m^2-t$ to the $\alpha$ contour of integration at $\alpha=0$. There is no pinch at this point. A pinch can only develop if one of the poles slips over to the other side of the countour at an end point. Hence to locate the singularities of $I_3^+$ due to the $\alpha$-pinch singularity one examines the singularities of $I_3^+$ generated by the $\alpha$-end-point singularities and determines for what values of $t$ that $\alpha$-end-point singularity is generated by a confluence of $\alpha$ poles at that end point. It is from such points on $I_3^+$ singularity curves that the $\alpha$-pinch-generated $I_3^+$ singularities emerge onto the physical sheet. For example the $\alpha=-1$ end-point singularity generates with the kinematic singularity at $x=0$ a branch point at $s=-12m^2$ for $m=\mu$. There is a confluence of poles at $\alpha=-1$ when $t=6m^2$. At this point $(s,t)=(-12m^2, 6m^2)$ a singularity on the curve

$$t^2+3\phi^2t-\frac{\phi^2}{m^2}(\tfrac{1}{4}s)^2=0 \quad (28)$$

emerges onto the physical sheet. This singularity is generated by an $\alpha$-pinch singularity in confluence with the pole at $x=0$. The equation is obtained from (26) and (27) by substituting $v=-m^2$ and eliminating $u$. It eventually moves into the complex plane.

New singularities of $I_3^+$ arise from the $\alpha$-pinch singularity at the end point of the $x$ integration. These occur at $s=0, m^2$ and are weak of order $\Delta^2\ln\Delta$ where $\Delta$ is the distance from the singularity. From the branch point at $s=0$ emerges a singularity on the curve

$$t=\tfrac{3}{2}m^2-(\tfrac{1}{4}s-m^2)(3s/m^2)^{1/2} +\frac{1}{2m}[(s+5m^2)(3m^2-s)\sqrt{s}\,(\sqrt{3}\,m-\sqrt{s}\,)]^{1/2} \quad (29)$$

for $m=\mu$ at $(s,t)=(0,\frac{3}{2}m^2)$. It is generated by a confluence of $\alpha$-pinch singularities in the $x$ plane. It eventually moves into the complex plane.

$B_2^{\mathrm{CH}}$ ($B_2^{\mathrm{EA}}$) is essentially a linear combination of $I_1^+, I_3^+$ ($I_3^+, I_2^+$), and hence the singularity structure of $B_2^{\mathrm{CH}}$ and $B_2^{\mathrm{EA}}$ can now be deduced from our analysis.

We present the results in Fig. 2, where we plot the singularities of the four second Born terms.

## IV. THREE-PARTICLE UNITARITY

The two types of model satisfying two- and three-particle unitarity that have been studied numerically we will refer to as the field-theory model[6] and the generalized Lippmann-Schwinger[1,2] model – both models are essentially *ad hoc*. The field-theory model is a linear integral equation for the sum of the minimum number of Feynman graphs that will yield two- and three-particle unitarity. The integral operator involves integration over relative energy. In the generalized Lippmann-Schwinger model the relative energy has been removed by an *ad hoc* mutilation of the Green's function propagator yielding a minimal extension off shell satisfying unitarity.

In this section we wish to show how by a consistent procedure one may derive from a field-theory model a generalized Lippmann-Schwinger model. The field-theory model is given by Eq. (5)

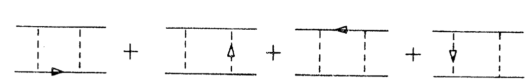

FIG. 4. Representation of a method to evaluate the Feynman integral of a box graph.

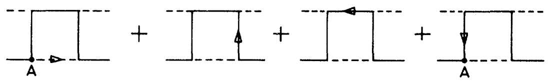


FIG. 5. Representation of a method to evaluate the Feynman integral of a box graph.

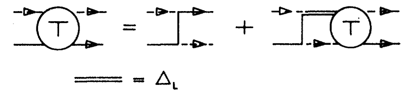


FIG. 6. Pictorial representation of Eq. (35).

provided we replace the propagators $D_{\pm}^{-1}$ by dressed propagators that possess at least two-particle branch cuts. Summing the simplest nonoverlapping set of bubble graphs does not lead to a consistent scheme, since the particle pole is shifted to the renormalized position but the two-particle branch point is not so renormalized. Saenger[6] has considered a summation over a larger number of graphs and as a consequence has proposed a nonlinear equation for the dressed propagator

$$\Delta_s(p^2) = [p^2 - m_0^2 - \Sigma(p^2)]^{-1}\ , \tag{30}$$

where

$$\Sigma(p^2) = \frac{i\lambda}{2\pi}\int d^4k\, \Delta_s(k^2)[(p-k)^2 - \mu^2]^{-1}\ , \tag{31}$$

which can be solved by iteration.[6] More simply one can use the propagator of Levine *et al.*,[6]

$$\Delta_L(p^2) = (p^2 - m^2)^{-1}[1 + (p^2 - m^2)\Sigma_2(p^2)]^{-1}, \tag{32}$$

where

$$\Sigma_2(p^2) = \lambda \int_{(m+\mu^2)}^{\infty} ds\, \rho(s)(s - m^2)^{-2}(s - p^2 - i\epsilon)^{-1} \tag{33a}$$

and

$$\rho(p^2) = \int d^4k\, \delta^+(k^2 - m^2)\delta^+((p-k)^2 - \mu^2)\,. \tag{33b}$$

To prevent ghosts one must impose an upper bound on the coupling constant of $\Sigma_2$.

The energy-analytic method does not naturally lead to a three-particle unitary model. Instead we will use the method of Gross which is based on a certain procedure for evaluating Feynman integrals. For the box diagram the procedure is as follows. The integral to be evaluated is

$$\int d^4k\{[(k-p)^2 - \mu^2][(k+\tfrac{1}{2}E)^2 - m^2] \times [(k-\tfrac{1}{2}E)^2 - m^2][(k-q)^2 - \mu^2]\}^{-1}\,. \tag{34}$$

Completing the contour in the upper half-plane of $k_0$ and using the residue calculus, we obtain four terms corresponding to the four graphs of Fig. 4, where the line with a full-headed arrow denotes an on-mass-shell $\delta$ function. The dominant term for $\mu/m$ small is the first (Fig. 4). The simplest way to see that this is true is to note that for $\mu = 0$ the first term diverges while the other three stay finite. Gross studied the higher-order planar and nonplanar ladder graphs in a similar fashion and wrote the sum of the dominant terms as a two-particle unitary model which when restricted to planar graphs is given by Eq. (2).

We use this method to obtain a simple model for a "spinless $N$-$\pi$" system where the potential is given by an exchanged nucleon propagator.[1] The box diagram of this system evaluated by completing the $k_0$ contour in the upper half-plane is given by the four terms represented by the graphs of Fig. 5. A measure of the relative size of these four terms is given by the separation between the singularities and the integration surface. For example, in comparing the first and fourth terms at vertex $A$ with external particles on the mass shell, it is clear that the meson in the fourth term (Fig. 5) is further off shell than the nucleon in the first term. In other words, the meson singularity in the fourth term is further from the integration surface than the nucleon singularity in the first term. A rough measure of the distance off shell is given by the deficiency index ($d$) of a vertex defined by $d = \min|m_1 \pm m_2 \pm m_3|$, where $m_1$, $m_2$, $m_3$ are the masses of the particles at the vertex. Thus for vertex $A$ of the first (fourth) term $d = \mu$ ($d = 2m - \mu$). Analysis of the second and third terms indicates that the first term is dominant overall.

This result still stands if we replace the bare nucleon propagators by dressed propagators of the form (30) or (32). Analysis of higher-order dressed planar ladder graphs in the manner of Gross leads to the following integral equation for the dominant terms:

$$T(k_1, p_1 | k_2, p_2) = T_0(k_1, p_1 | k_2, p_2) + \lambda \int d^4k [(p_1 + k)^2 - m^2]^{-1} \Delta_L((p_1 + k_1 + k)^2) \times \theta(-k_0)\delta(k^2 - \mu^2) T(-k, p_1 + k_1 + k | k_2, p_2)\,. \tag{35}$$

If one had used propagator (30) then the nucleon exchange propagator would also have to be dressed. A graphical representation of Eq. (35) is given in Fig. 6. With $k_1$ on mass shell, Eq. (35) is explicitly a relativistic equation without relative energy.

We finally prove that Eq. (35) satisfies unitarity in the elastic and first inelastic regions.[18,19] If we write Eq. (35) as

$$T = T_0 + KT \tag{36}$$

and subtract its complex conjugate, we obtain

$$T - \overline{T} = T_0 - \overline{T}_0 + (K - \overline{K})\overline{T} + K(T - \overline{T}) . \tag{37}$$

Considering $(K - \overline{K})\overline{T}$ as the inhomogeneous term, we obtain

$$T - \overline{T} = R(T_0 - \overline{T}_0) + R(K - \overline{K})\overline{T} , \tag{38}$$

where $R = (I - K)^{-1}$. In the elastic region $T_0 = \overline{T}_0$ and

$$\begin{aligned} \text{kernel}\,(K - \overline{K}) &= -2\pi i \lambda [(p_1 + k)^2 - m^2]^{-1} \delta^+((p_1 + k_1 + k)^2 - m^2)\delta^+(k^2 - \mu^2) \\ &= -i(2\pi)^{-2} T_0 \delta^+((p_1 + k_1 + k)^2 - m^2)\delta^+(k^2 - \mu^2) . \end{aligned} \tag{39}$$

But $RT_0 = T$; hence two-particle unitarity follows.

In the first inelastic region $T_0 = \overline{T}_0$, and the kernel of $(K - \overline{K})$ is given by

$$\begin{aligned} &-2\pi i \lambda \delta^+(k^2 - \mu^2)\{\delta^+((p_1 + k)^2 - m^2)\,\overline{\Delta}_L((p_1 + k_1 + k)^2) \\ &\qquad + [(p_1 + k)^2 - m^2]^{-1}\,\delta^+((p_1 + k_1 + k)^2 - m^2) + [(p_1 + k)^2 - m^2]^{-1}\lambda \Delta_L \overline{\Delta}_L \rho((p_1 + k_1 + k)^2)\} . \end{aligned} \tag{40}$$

With the identification of the two-three-particle amplitude as

$$T(k_1, p_1 | k_2, p_2)\Delta_L(p_2) v(p_2; k_3, p_2 - k_3) , \tag{41}$$

and $v$ taken to be bare, substitution of (40) in (38) leads to the unitarity relation in the first inelastic region.

In a further paper we hope to consider a generalization of this model incorporating time invariance, nonplanar contributions, and spin.

---


[1] R. Aaron, R. D. Amado, and Y. Y. Yam, Phys. Rev. 140, B1291 (1965); R. Aaron and R. D. Amado, *ibid.* 150, 857 (1966); R. Aaron, R. D. Amado, and J. E. Young, *ibid.* 174, 2022 (1968); R. Aaron, D. Teplitz, R. D. Amado, and J. E. Young, *ibid.* 187, 2047 (1969).

[2] D. Freedman, C. Lovelace, and J. Namyslowski, Nuovo Cimento 43, 258 (1966).

[3] R. Blankenbecler and R. Sugar, Phys. Rev. 142, 1051 (1966).

[4] H. Bethe and E. E. Salpeter, Phys. Rev. 84, 1232 (1951); M. Gell-Mann and F. E. Low, *ibid.* 84, 350 (1951); J. Schwinger, Proc. Natl. Acad. Sci. U.S. 37, 455 (1951).

[5] H. Cohen, Phys. Rev. D 2, 1738 (1970).

[6] M. Levine, J. Wright, and J. Tjon, Phys. Rev. 154, 1433 (1967); 157, 1416 (1967); R. Saenger, *ibid.* 159, 1433 (1967).

[7] O. I. Zav'yalov, M. K. Polivanov, and S. S. Khoruzhii, Zh. Eksp. Teor. Fiz. 45, 1654 (1963) [Sov. Phys. JETP 18, 1135 (1964)].

[8] J. L. Basdevant and R. L. Omnès, Phys. Rev. Letters 17, 775 (1966).

[9] A. A. Langunov and A. N. Tavkhelidze, Nuovo Cimento 29, 380 (1963).

[10] J. V. Greenman, Nuovo Cimento 65B, 174 (1970).

[11] D. Amati, A. Stanghellini, and S. Fubini, Nuovo Cimento 26, 896 (1962); L. Bertocchi, S. Fubini, and M. Tonin, *ibid.* 25, 626 (1962).

[12] N. Nakanishi, Progr. Theoret. Phys. (Kyoto) Suppl. 43, 1 (1969).

[13] F. Gross, Phys. Rev. 186, 1448 (1969).

[14] H. Cohen, A. Pagnamenta, and J. G. Taylor, Nuovo Cimento 50, 796 (1967).

[15] J. G. Taylor, in *Lectures in Theoretical Physics: Mathematical Methods of Theoretical Physics,* edited by W. E. Brittin *et al.* (Gordon and Breach, New York, 1967), Vol. IXA; A. Pagnamenta and J. G. Taylor, Phys. Rev. Letters 17, 218 (1966).

[16] R. G. Newton, *Scattering Theory of Waves and Particles* (McGraw-Hill, New York, 1965), p. 292.

[17] R. J. Eden, P. V. Landshoff, D. I. Olive, and J. C. Polkinghorne, *The Analytic S-Matrix* (Cambridge Univ. Press, Cambridge, 1966).

[18] J. V. Greenman, Commun. Math. Phys. 16, 123 (1970).

[19] V. A. Alessandrini and R. L. Omnès, Phys. Rev. 139, B167 (1965).